

Localized Corrosion Resistance and Cytotoxicity Evaluation of Ferritic Stainless Steels for Use in Implantable Dental Devices with Magnetic Connections

Rogério Albuquerque Marques^{*}, Sizue Ota Rogero, Maysa Terada, Eurico Felix Pieretti, Isolda Costa

Centro de Ciência e Tecnologia de Materiais, Instituto de Pesquisas Energéticas e Nucleares (CCTM-IPEN), Av. Prof. Lineu Prestes, 2242, São Paulo, 05422-970, Brazil,

*E-mail: rogeriomarques_99@yahoo.com

Received: 6 September 2013 / Accepted: 18 November 2013 / Published: 5 January 2014

The ferromagnetic property of ferritic stainless steels makes them potential materials for use as implantable dental devices with magnetic connections. In this work, the corrosion resistance and cytotoxicity of the AISI 444 ferritic stainless steel (SS) was evaluated in a phosphate buffer solution (PBS) and compared with two materials used for fabrication of implantable materials, specifically, NeoM (a ferritic type of SS) and ISO 5832-1 (an austenitic type of SS). All tested materials showed passivity in the PBS electrolyte used. Susceptibility to pitting corrosion in the test solution used however was only associated to the NeoM steel, that has been used in commercial dental implant devices. A large concentration of precipitates/inclusions of complex nature was found in the microstructure of this steel and it is the probable reason for its low resistance to localized corrosion, much lower than that of the AISI 444 SS used in this study. The AISI 444 stainless steel tested is a Nb and Ti stabilized steel and it presented mainly Nb and Ti rich types precipitates in its microstructure. No pits were seen at the surface of this last steel after polarization tests. The pitting resistance of the AISI 444 steel was compared to that of the ISO 5832-1 austenitic and it was found similar to this last steel that is well known for its good corrosion resistance performance. The results suggested that the AISI 444 steel is a potential candidate for replacement of the commercial ferromagnetic alloys currently used in dental prosthesis.

Keywords: Biomaterials, Corrosion, Dental Prosthesis, Ferritic Stainless Steels, AISI 444.

1. INTRODUCTION

Many metallic alloys are widely used in the medical and dental care due to their physicochemical properties. Many properties are required during the interaction of these alloys with

the human body such as good mechanical performance, wear resistance, and corrosion resistance in the body fluids they are exposed to. In many applications, the absence of ferromagnetism is another obligatory property. Among the metallic biomaterials, the stainless steels (SS) are currently the most extensively used, corresponding to over 50% of the total market [1].

The outstanding corrosion resistance of stainless steels results from a thin and protective passive film, which acts as a partial barrier between the metal and the corrosive species present in the environments they are in contact. However, aggressive anions such as chlorides present in the body fluids may interact with the passive film leading to a locally increased dissolution rate. The stability of the passive film when it is exposed to aggressive species is of essential importance in order to prevent localized corrosion [2].

Among the stainless steels, the most common material used in the manufacture of orthopedic prostheses is the austenitic stainless steel ASTM F138. One of the requirements of this standard is the absence of ferromagnetism, which could cause dislocation of the prosthesis, if the patient undergoes MRI exam. Nevertheless, the ferromagnetism typical of ferritic SS is necessary for some specific applications, such as magnetic connectors, to stabilize dental and facial prosthesis, in the manufacture of orthodontic brackets, and even in the manufacturing of dialysis machines [3]. Certain grades of ferritic SS such as SUS 444, SUS XM27, and SUS 447J1 have been successfully tested for making prosthetic magnetic connectors [4,5].

Frederick *et al.* [6] were pioneers in the proposal of prosthesis fixation by magnetism. They described the fabrication of prosthesis with magnetic connection to a patient operated for a jaw infiltrated carcinoma, who had lost part of the palate and the right orbit. The prosthesis was made in two parts, one placed through the mouth and the other by the orbit. The union between them occurred due to the attraction between the magnets positioned in each segment of that prosthesis.

Gillings [7] designated the clinical and laboratory procedures for the use of permanent magnets for dental prostheses retention. The results showed that the magnetic prosthesis can be an economical alternative to dental extraction.

Highton *et al.* [8] conducted tests *in vitro* to evaluate the retention characteristics of a magnetic implant. It was shown that even after 44 000 cycles of withdrawal and replacement of the prosthesis, the magnets did not lose their retentive strength, unlike the systems based on frictional holding, showing advantage over conventional systems.

In comparison with the systems of prostheses that are fixed by mechanical retention, the magnetic retention has advantages, such as the reduction of non-axial or lateral forces, which are detrimental to bone tissue by inducing the reabsorption process. A flat surface between the magnet and the prosthetic connector allows rotation during the function, improving the prognosis [9]. In addition, other advantages associated to the magnetic retention are the easy positioning of the magnet, taking into account that there is no need for a parallel insertion axis between the components set in the mouth [10]; and the facility of placement and hygiene, especially in patients with some type of motor impairment. Due to such advantages, ferritic SS have been evaluated as materials for use in dental prostheses with magnetic retention.

Okuno *et al.* [11] studied the corrosion resistance of some ferritic SS used in magnetic connections, specifically SUS447J1 and SUS444 systems, by means of potentiodynamic polarization

curves and open circuit potential measurements as a function of time of immersion in a solution of 0.9 (wt.%) NaCl at 37 °C. The SUS 316L SS was selected as control material once it is a widely used material for implants fabrication. Their results showed that the ferritic stainless steels studied exhibit higher pitting corrosion resistance than the SUS 316L SS. The SUS447J1 SS showed corrosion resistance superior to the SUS444 SS.

Despite of the good resistance of the ferritic stainless steels investigated to date, research work carried out in our laboratory found that materials that are not according to standards have been used in commercial implants. The use of these materials could lead to undesirable corrosion with the consequent liberation of corrosion products into the body fluids and premature failure.

The aim of this work was to evaluate the corrosion resistance of a commercial implant made of a ferritic SS and compare its performance with that of the commercial AISI 444 ferritic SS. This last material was not obtained from a commercial implant piece but was provided as a plate. The properties evaluated were the cytotoxicity, magnetic retention force, and corrosion resistance by electrochemical methods.

2. EXPERIMENTAL

The surfaces of the AISI 444 ferritic SS and ISO 5832-1 austenitic SS, whose chemical composition is shown in Table 1, were prepared for microstructure and electrochemical characterization by grinding and polishing, in the as received condition. For comparison reasons, the surface of a commercial magnet component called NeoM was also prepared for microstructure and corrosion resistance evaluation (Figure 1).

The microstructure and chemical semiquantitative characterization of the tested materials were carried out by scanning electron microscopy (SEM) and energy dispersive spectroscopy (EDS).

The chemical composition of the NeoM material used in this study was evaluated and compared with the nominal composition, both shown in Table 2.

Table 1. Chemical composition (wt.%) of the AISI 444 (ferritic) and ISO 5832-1 (austenitic) stainless steels tested.

	Cr	Ni	Mo	Mn	Si	Nb	Ti	N	S	C	Fe
ISO 5832-1	18.32	14.33	2.59	2.09	0.37	0.33	0.009	0.047	0.008	0.023	bal.
AISI 444	16.27	0.50	1.99	0.13	0.58	0.13	0.11	0.04	0.015	0.013	bal.

Table 2. Nominal and analyzed composition of the NeoM SS used in this investigation.

NeoM	Cr	Ni	Mo	Mn	Si	Nb	Ti	N	S	C	Fe
Nominal	17.5- 19.5	≤1.0	1.75- 2.50	≤1.0	≤1.0	≤0.025	≤0.030	≤0.04	≤0.8	≤0.025	bal.
Analyzed	13.2	3.11	0.34	1.34	1.10	*	*	0.04	0.30	*	bal

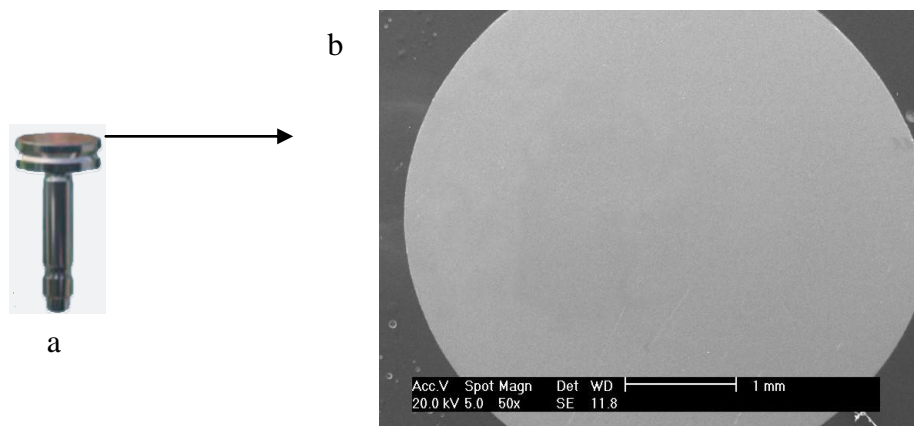


Figure 1. (a) NeoM magnet component used and (b) polished surface used for microstructure and electrochemical characterization.

The cytotoxicity of the AISI 444 SS was evaluated in the present study according to Rogero *et al.* [12] and ISO 10993- 5 [13] by immersion of samples of the SS in Minimum Essential Medium (MEM) at 37 ° C for 10 days.

The electrochemical tests were performed in a phosphate buffered solution (PBS), naturally aerated, at pH 7 and 37 ° C. The chemical composition of the PBS is shown in Table 3. The electrochemical tests used consisted in cyclic potentiodynamic polarization, after 2 and 21 days of immersion in the PBS solution (Table 3).

Table 3. Chemical composition (wt. %) of the phosphate buffer solution (PBS) used.

NaCl	Na ₂ HPO ₄	KH ₂ PO ₄
0.9	0.142	0.272

The electrochemical tests were carried out using a three electrode set-up arrangement and a Gamry PCI4/300 equipment, with a Pt counter electrode (wire with a geometric area of 2.0 cm²) and an Ag/AgCl (3M) reference electrode. All the potentials will be referred to the Ag/AgCl (3M) reference electrode. The area of the working electrode exposed to the electrolyte corresponded to 1 cm². Cyclic polarization tests were performed with a scan rate of 1.0 mV/s. The electrochemical tests were repeated four times to evaluate reproducibility and the mean values of the pitting potentials. The standard deviation was estimated from these results.

3. RESULTS AND DISCUSSION

3.1. Surface Characterization

Surface characterization of the AISI 444 was carried out by SEM and a micrograph of this steel after metallographic etching using Villela’s solution is shown in Figure 2, showing the presence of few and small and precipitates located inside the grains.

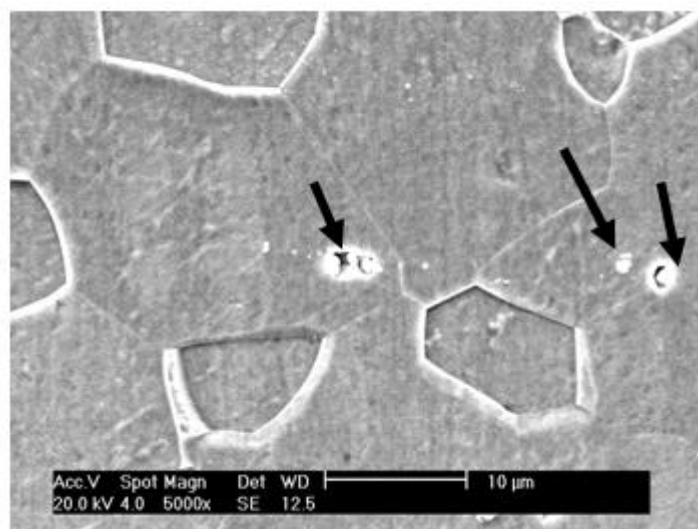
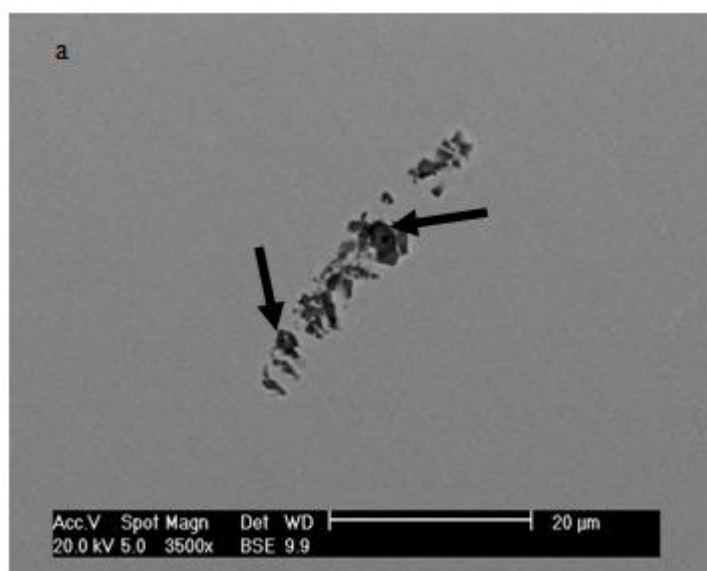


Figure 2. SEM micrograph of AISI 444 SS after metallographic etching with Vilella's solution showing few precipitates located inside the grains.

The surface of the AISI 444 SS was also observed by SEM after surface finishing by polishing but without etching in search for heterogeneities, such as precipitates or defects, that could lead to localized corrosion were analyzed by EDS. Figure 3 (a) shows a defect at the surface that seems to be associated to a cold deformation process. Some precipitates were seemingly trapped inside the defect. These precipitates were rich in titanium but also nitrogen and niobium were detected in the corresponding EDS spectrum, as Figure 3 (b) illustrates. In the stabilized type of SS tested, Nb and Ti are added to prevent the formation of chromium carbides or nitrides, avoiding chromium impoverishment in the matrix.



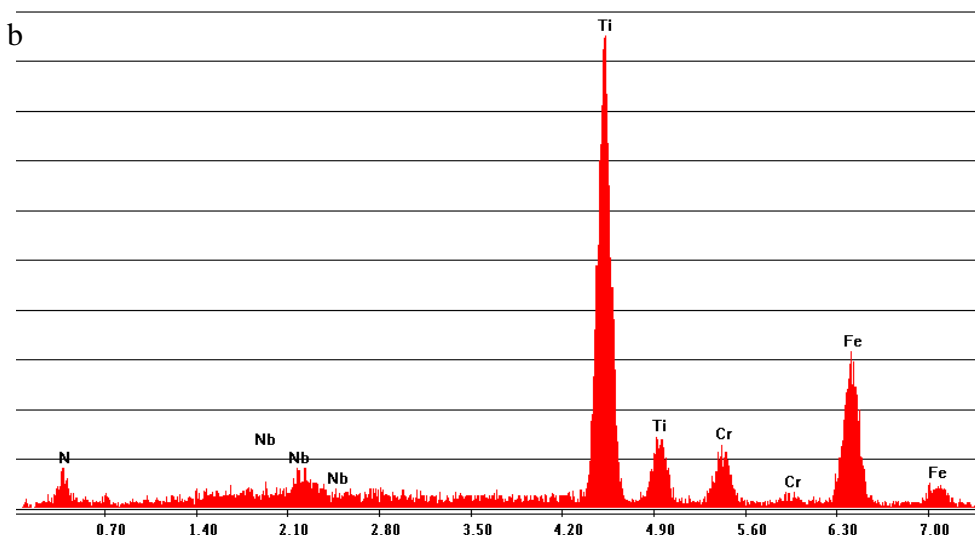


Figure 3. (a) SEM image of the AISI444 SS tested showing surface defects and precipitates associated to them and (b) corresponding EDS spectrum showing a Ti and Nb enriched area.

As niobium and titanium have greater affinity with carbon than chromium, nitrides carbides of these elements were preferentially formed. The formation of nitrides instead of carbides might be explained by the higher nitrogen content in this steel comparatively to that of carbon. These precipitates only dissolve in the ferritic matrix at temperatures above 1200 °C. Consequently, the stabilized steels tend to maintain a completely ferritic structure until the melting temperature, besides maintaining the corrosion resistance of the stainless steel [14]. These results show that Ti and Nb addition into the AISI 444 were effective in keeping the Cr in solution. Besides, manganese sulphide inclusions were not found on this steel due to the very low manganese and sulphur content in its composition.

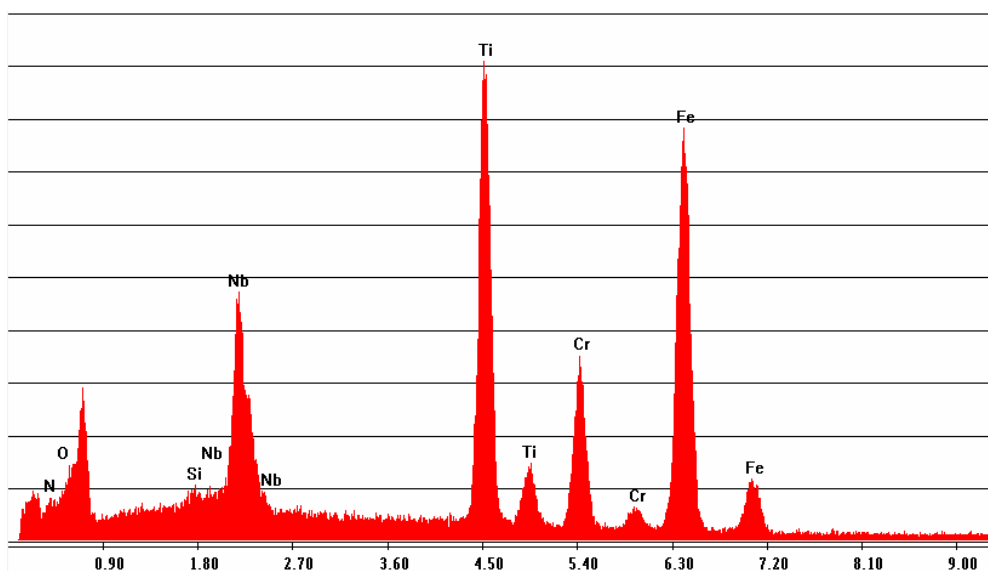
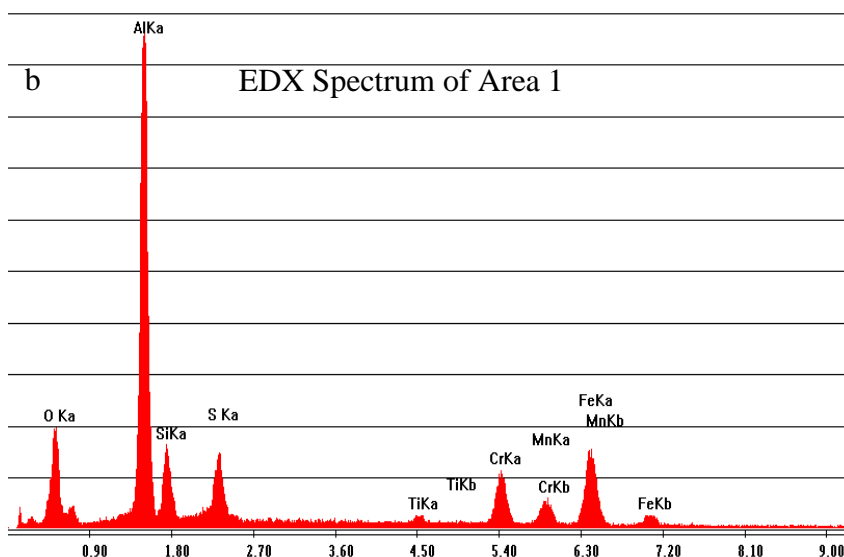
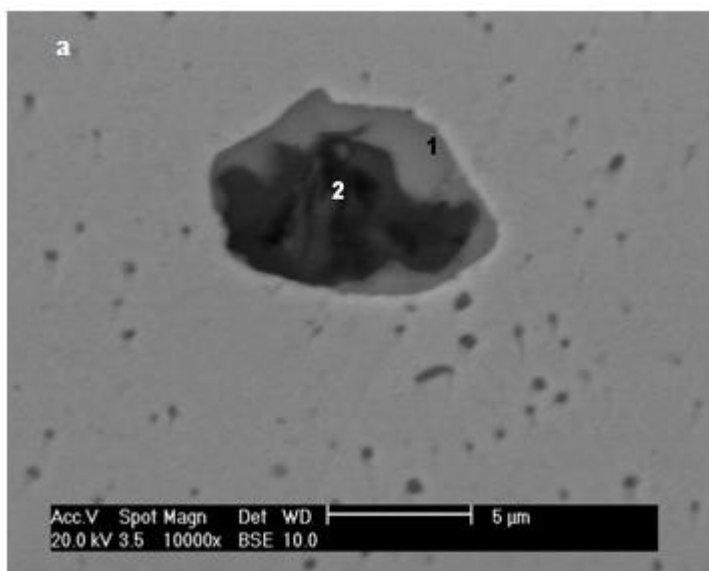


Figure 3. EDS spectrum of a precipitate rich in Ti and Nb on the AISI 444 SS.

EDS spectrum obtained on another particle also showed it was Ti and Nb rich, as Figure 4 confirms. The characterization results show that the precipitates found in the AISI 444 SS tested consisted mainly of Ti and Nb rich types and they are inside the grains.

Figure 4 shows a large precipitate in the NeoM SS and a large number of small precipitates surrounding it. The large precipitate is composed of two parts of different compositions. The EDS spectrum corresponding to each of these areas suggests that it is a mixed oxide/sulphide precipitate, as Figures 4 (b) and (c) indicate. Another type of large precipitate found in the NeoM tested with different morphology from that shown in Figure 4 was seen at the surface of the NeoM SS, and this is presented in Figure 5. The EDS spectrum indicates it is a manganese sulphide inclusion type that might also contain chromium. The small precipitates around the elongated inclusion were not analyzed due to their small sizes leading to matrix composition interference in the result of analysis.



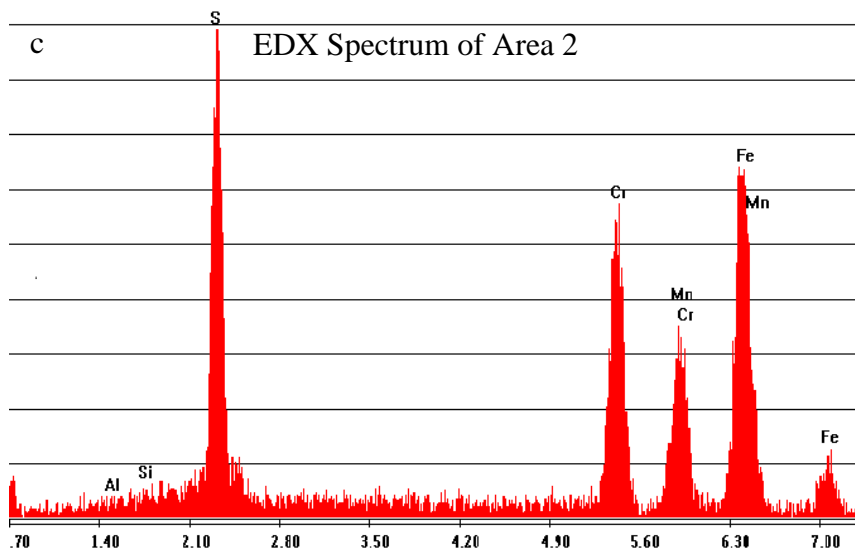


Figure 4. (a) SEM micrograph of the surface of the NeoM stainless steel tested showing a large precipitate surrounded by a large number of small ones. (b) EDS spectrum of the area marked as 1, and c) EDS spectrum of the area of area marked as 2.

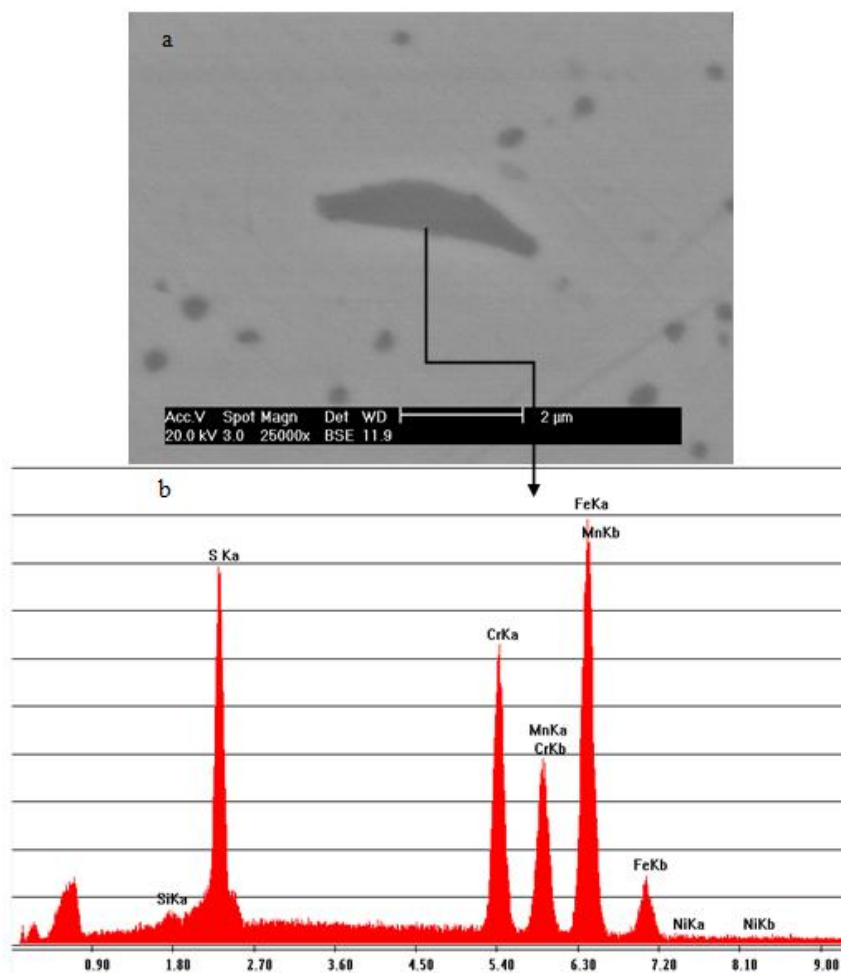


Figure 5. (a) SEM micrograph of the surface of the commercial NeoM stainless steel showing an elongated precipitate (b) EDS spectrum of the precipitate shown in (a) indicates it is a manganese sulphide type.

3.2. *In vitro* cytotoxicity analysis

In order to investigate the cytotoxicity of the AISI 444 SS, *in vitro* cytotoxicity analyses was performed using the neutral red incorporation method, as Figure 6 shows.

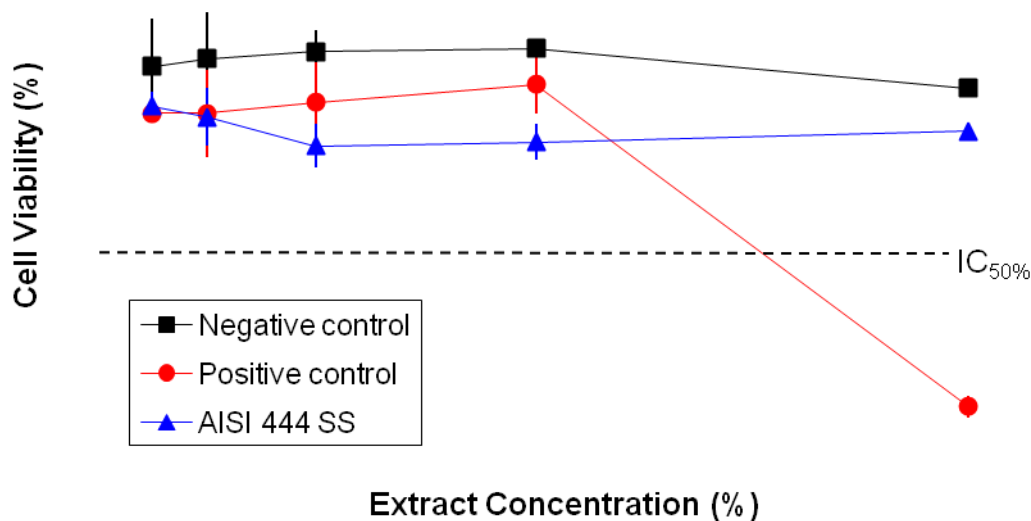


Figure 6. *In vitro* cytotoxicity assay for the AISI 444 SS.

The results presented in Figure 6 show that the AISI 444 SS exhibited behavior similar to the negative control, that is, it shows no cytotoxicity. This is indicated by the cell viability curve for the AISI 444 SS above the level $IC_{50\%}$ of cytotoxicity.

3.3. Potentiodynamic Polarization Curves

The results of the polarization curves showed reproducibility and the curves presented in Figure 7 are representative of these results. Figures 7 (a) and (b) compare the anodic polarization curves of the ISO 5832-1 (austenitic) and the AISI 444 (ferritic), and the AISI 444 and NeoM stainless steels, respectively, after 2 days of immersion in the PBS test solution.

The polarization curves show that the AISI 444 and the ISO 5832-1 SS presented analogous corrosion resistance with similar anodic currents during the whole range of polarization. The increase in current that occurred at potentials around $(1.10 \pm 0.05) V_{Ag/AgCl}$ could be due to the oxygen evolution reaction or to the film breakdown with the nucleation of pitting. The NeoM SS, however, showed much higher susceptibility to film breakdown than the other steels studied. The potential related to film breakdown corresponded to $(0.45 \pm 0.10) V_{Ag/AgCl}$ but pits nucleation started at even lower potentials. The hysteresis seen at the reverse polarization curve of this material, show its low tendency to repassivation.

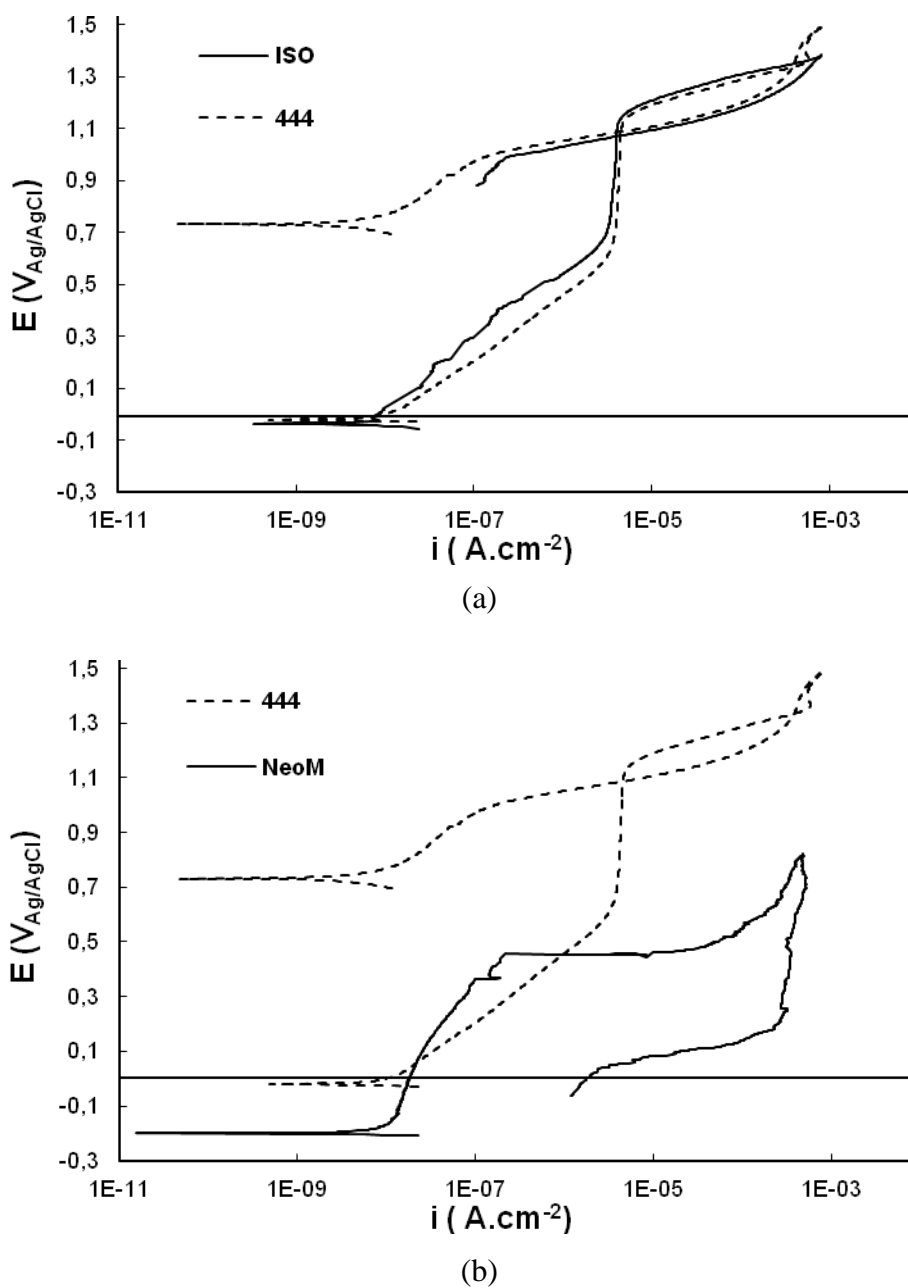


Figure 7. Polarization curves of the tested steels in PBS solution after 2 days of immersion. (a) comparison of AISI 444 and ISO 5832-1 and (b) comparison of the AIS 444 and NeoM.

Polarization curves for the NeoM SS were also obtained after 21 days of immersion in the PBS solution and a comparison of the curves corresponding to 2 and 21 days of immersion are presented in Figure 8. The lower current densities in the passive region and the higher corrosion and breakdown potentials for the sample immersed during 21 days in the PBS comparatively to that exposed to the electrolyte for 2 days indicate that the thickness of the passive film has increased between 2 and 21 days of exposure in the test solution. However, the results also show a greater area of hysteresis associated to the sample immersed for 21 days, showing that once the passive film related to this

specimen is broken, it is more difficult to repassivate than in the sample with a thinner film. This could be related to breakdown of the passive film at fewer points leading to deeper penetration of the localized corrosion in the case of the sample immersed for longer periods.

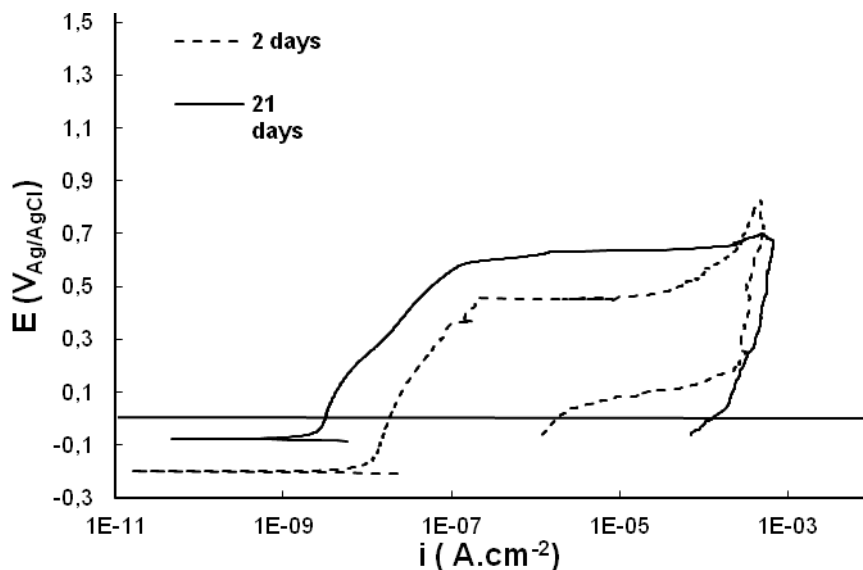
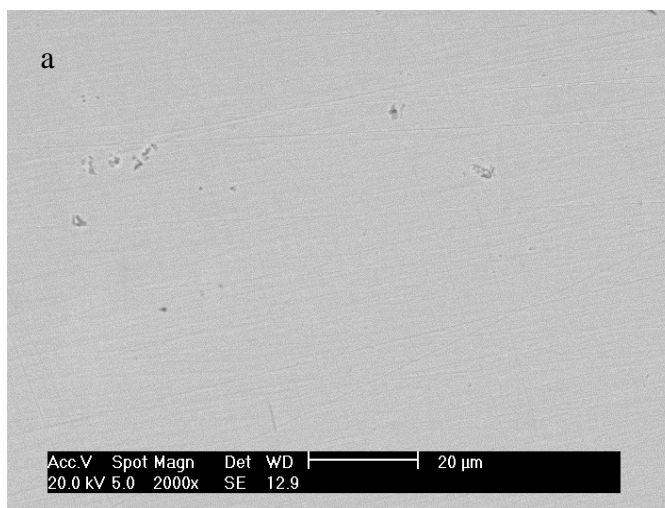


Figure 8. Comparison of the polarization curves of the NeoM stainless steel after 2 and 21 days of immersion in PBS solution.

The surfaces of the AISI 444 and NeoM were observed after the polarization tests and no evidence of pits at the surface was found associated to the AISI 444 SS, as Figure 9 (a) shows. This result supports the hypothesis that the increase in current was related to the oxygen evolution reaction. The increase in current for the NeoM that occurred at potentials around $(0.45 \pm 0.10) V_{Ag/AgCl}$ for the sample immersed during 2 days in the PBS, however was due to the passive film breakdown and the formation of pits, as illustrated in Figure 9 (b). A large number of pits were found at the polarized surface of the NeoM SS and the hysteresis seen the polarization curve during the reverse direction of polarization, shown in Figure 8, indicates that the pits do not present propensity to repassivate.



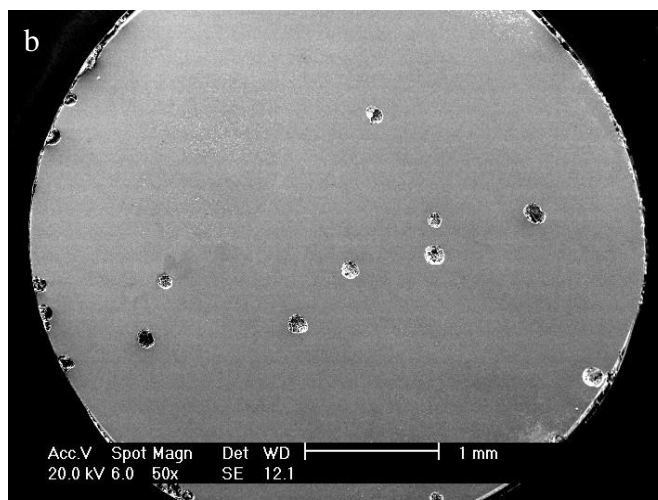
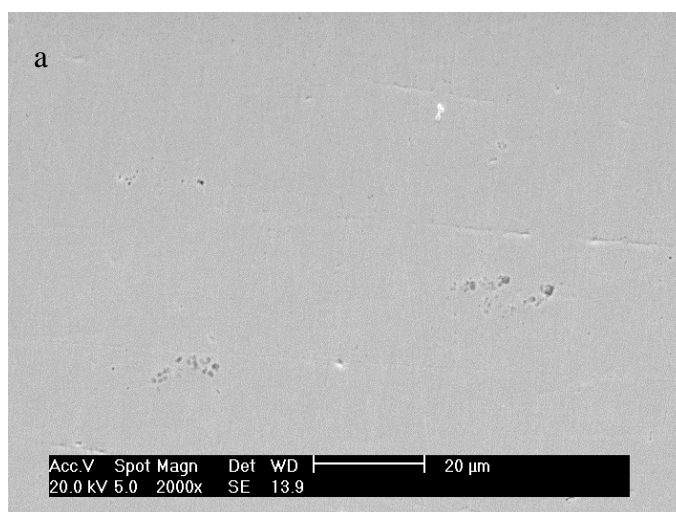


Figure 9. (a) Surface of the AISI 444 SS and (b) NeoM SS, after polarization test carried out after 2 days of immersion in the PBS solution.

Similar behavior was also observed for the same steels polarized after 21 days of immersion in PBS, as seen in Figure 10. After this period of immersion followed by polarization pits still were not found at the surface of the AISI 444. On the other hand, for the NeoM SS, film breakdown occurred at potentials of $(0.55 \pm 0.10) V_{Ag/AgCl}$ which is superior to the film breakdown potential obtained for the NeoM samples that had been immersed for 2 days in the test solution. Besides, lower passive current densities were associated to the samples immersed for longer periods showing that the passive film had grown in thickness from 2 to 21 days of immersion. However, a larger area of hysteresis was related to the samples immersed for longer periods. This could be caused by the anodic current density being located at fewer areas for the samples with thicker passive films, preventing pit repassivation and leading to deeper pits at the surface, as surface observation after polarization suggested. As it was shown in the results of the present study, the AISI 444 ferritic SS was resistant to pitting whereas the NeoM ferritic SS showed low pitting resistance.



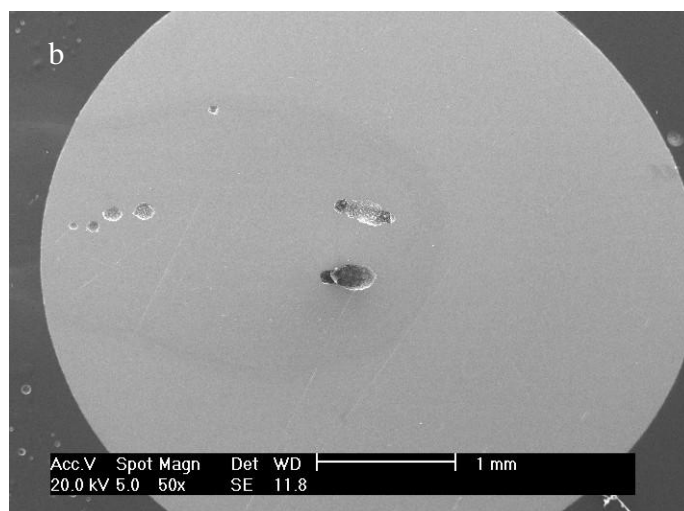


Figure 10. Surface of the (a) AISI 444 SS and (b) NeoM SS, after polarization test carried out after 21 days of immersion in the PBS solution.

The role of chloride ions on pitting susceptibility of various alloys has been widely investigated in literature [15-18].

It is well accepted that pitting initiates from a local breakdown of the passive film and the consequent formation of electrochemical cells in which the passive areas act as cathodes whereas the exposed metallic surface as anodes [19,20]. The stability of the initiated pit has been associated to the development of the chemistry at the bottom of the pit that leads to the pH decrease.

It has been proposed in literature [21] that the pit stability depends on the factor $x \times i$, where x is the pit depth and i is the pit current density. According to literature [15], when the stability product is larger than 3 mA cm^{-1} , the pit propagates in stainless steel.

It is widely accepted that the chloride ions (Cl^-) preferentially adsorb and accumulate at the imperfect/defective sites, resulting in initiation and propagation of pitting corrosion in steels [22]. Investigation using electron microprobe analyzer carried out to investigate the origins of the preferential Cl^- adsorption and pitting corrosion showed that pitting corrosion initiated and propagated at inclusions of MnS, where chloride ions preferentially adsorbed and accumulated leading to the conclusion that manganese sulfide inclusions are the most susceptible defects to pitting corrosion in chloride-containing solution [22]. Pitting corrosion nucleates at MnS inclusions [23].

The probability of initiation of pitting corrosion in stainless steels seems to be strongly dependent on the composition, density, and size of the inclusions. It has been proposed that the electrochemistry of the inclusion and its boundary with the steel is critical for the stability of the steel against pitting corrosion [24, 25]. According to this interpretation, the dissolution occurs initially predominantly at the edge of the inclusion, despite of some occurrences of dissolution at particular places on the exposed interior of the inclusion. The initial dissolution of the inclusion leads to the precipitation of a crust of sulphur over the inclusion and on the surrounding steel [25]. Underneath this crust, a local acidic environment with high concentrations of sulphide and chloride, is formed. In this environment, the steel is unstable, so its passivity breaks down and the second phase of pitting

corrosion commences, in which the local environment is maintained as a consequence of the steel dissolution into a diffusionally restricted zone.

Based on the importance of the MnS inclusions to the initiation of pitting corrosion, the composition of the NeoM studied with large contents of manganese, four times superior to that of the AISI 444 stainless steel tested, is most likely responsible for the inferior resistance to pitting corrosion of the NeoM steel.

4. CONCLUSIONS

The AISI 444 stainless steel used in this study showed high resistance to localized corrosion. It was similar to that of an austenitic stainless steel, ISO 5832-1 SS, which is used in the fabrication of implants and also much superior to that of a ferritic stainless steel which has been used in the fabrication of commercial magnet component of implants. The chemical compositions of the both ferritic stainless steels used are the reason for the results.

ACKNOWLEDGEMENTS

The authors are thankful to FAPESP (Proc. No. 2012/50288-8) for the financial support to this research.

References

1. World Biomedical Metal Market. Acmite Market Intelligence, February, 2010. Available in: <http://www.acmite.com/brochure/Brochure-Biomedical-Metal-Market-Report.pdf>
2. J. B. Lee, *Mater. Chem. Phys.*, 99 (2006) 224.
3. 1802 Datasheet, General Datasheet of precision wire 1802, Sandvik, Sweden – Available in: <http://www.smt.sandvik.com/sandvik/0140/internet/se01598.nsf/idea?OpenForm&ParentUNID=33060426167A992BC1256ABC002A44E2>
4. Y. Takada, K Nakamura, K. Kimura, O. Okuno, *Int. Congress Ser*, 1284 (2005) 314.
5. K. Nakamura, Y. Takada, M. Yoda, K. Kimura, O Okuno, *Dent. Mater. J.*, 27 (2008) 203.
6. C. S. Frederick, F. L. Deng, T. W. Chow. *J. Prosthet. Dent.*, 91 (2004) 219.
7. B. R. D. Gillings, *J. Prosthet. Dent.*, 49 (1983) 607.
8. R. Highton, A. A. Caputo, M. Kinni, J. Matyas, *J. Prosthet. Dent.*, 60 (1988) 486.
9. G. Saygili, S. Sahmali, *J. Oral Sci.*, 40 (1998) 61.
10. A. D. Walmsley, *Dent. Update*, 29 (2002) 428.
11. O. Okuno, Y. Takada, M. Kikuchi, K. Kimura, The First International Conference on Magnetic Applications in Dentistry, 2002, Tokyo. The Japanese Society of Magnetic Applications in Dentistry. <http://wwwsoc.nii.ac.jp/jmd/international/1st/>
12. S. O. Rogero, A. B. Lugao, T. I. Ikeda, A. S. Cruz, *Mater. Res.* 6 (2003) 317.
13. ISO 10.993 - *Biological evaluation of medical devices* - part 5: Tests for cytotoxicity: *in vitro* methods, p. 1-7, 1992.
14. E. Folkhard, *Welding metallurgy of stainless steels*, Wien, New York: Springer-Verlag, (1988) 140.
15. G. T. Burstein, P. C. Pistotius, S. P. Mattin, *Corros. Sci.*, 35 (1993) 57.
16. D. E. Williams, C. Westcott, M. Fleishmann, *J. Electrochem. Soc.*, 132 (1985) 1804.
17. D. E. Williams, C. Westcott, M. Fleishmann, *J. Electrochem. Soc.*, 132 (1985) 1786.
18. G. S. Frankel, L. Stockert, F. Hunkeler, H. Boehni, *Corrosion*, 43 (1987) 429.

19. P. Angell, J. S. Luo, D.C. White, *Corr. Sci.*, 37 (1995) 1085.
20. J. W. Oldfield, W. H. Sutton, *Br. Corros. J.*, 13 (1978)13.
21. J. R. Galvele, *Corr. Sci.*, 21 (1981) 551.
22. B. Lin, R. Hu, C. Ye, Y. Li, C. Lin, *Electrochim. Acta*, 55 (2010) 6542.
23. J. Stewart, D. E. Williams, *Corros. Sci.*, 33 (1992) 457.
24. P. Schmuki, H. Hildebrand, A. Friedrich, S. Virtanen, *Corros. Sci.*, 47 (2005)1239.
25. D. E. Williams, T. F. Mohiuddin, Y. Y. Zhu, *J. Electrochem. Soc.*, 145 (1998) 2664.

© 2014 by ESG (www.electrochemsci.org)